VNU Journal of Science: Mathematics - Physics

Journal homepage: https://js.vnu.edu.vn/MaP

Original Article

Solving Problems with the Functionally Graded Anisotropic Piezoelectric Plates Via a BFEM

Nguyen Xuan Thanh[1,2], Nguyen Dinh Duc[1], Nguyen Van Thuong[1,*]

[1]*VNU University of Engineering and Technology, 144 Xuan Thuy, Cau Giay, Hanoi, Vietnam*

[2]*Thainguyen University of Technology, 666 - Road 3-2, Tich Luong, Thai Nguyen, Vietnam*

Received 10th March 2026
Revised 25th March 2026; Accepted 13th April 2026

Abstract: A boundary-based finite element method (BFEM) is developed for solving stress and contact problems in two-dimensional multilayered and functionally graded piezoelectric plates. In the proposed formulation, the plate is discretized into multiple material sublayers, each modeled as an individual finite element constructed solely from boundary nodes. By establishing direct relations between boundary tractions and electric displacements and nodal forces, the governing electromechanical coupling equations are transformed into a boundary-based finite element framework, thereby avoiding volumetric discretization. When contact problems are considered, the contact constraints are incorporated into the BFEM formulation through appropriate contact conditions, allowing the unknown contact regions and contact tractions to be determined as part of the solution. The proposed approach effectively accounts for multilayered configurations, functionally graded material properties, anisotropy, and electromechanical coupling effects. Numerical examples are presented to validate the method's accuracy and convergence. In addition, parametric studies are conducted to investigate the influences of material gradation and anisotropic properties on the electromechanical responses of the plates.

Keywords: BFEM, functionally graded, multilayered, anisotropic, piezoelectricity, contact analysis.

1. Introduction

Functionally graded and multilayered piezoelectric plates are widely utilized in smart and multifunctional structures, including sensors, actuators, energy harvesters, and adaptive mechanical systems [1-5]. By tailoring the material composition through the thickness or by stacking multiple

* Corresponding author.
E-mail address: thuong.nv@vnu.edu.vn

https//doi.org/10.25073/2588-1124/vnumap.5126

piezoelectric layers, these structures can achieve improved electromechanical performance, enhanced reliability, and reduced stress concentrations [4-7]. Accurate modeling of their electromechanical behavior is therefore essential for design and optimization in advanced engineering applications.

The analysis of anisotropic FG or multi-layered elastic/piezoelectric plates is challenging due to the strong coupling between mechanical and electrical fields, material anisotropy, and spatial variation of material properties [4-10]. These difficulties are further amplified when contact phenomena are involved, such as indentation, actuator-substrate interaction, or contact with external components [11-15]. Contact problems introduce additional nonlinearities in the form of inequality constraints, unknown contact regions, and coupled electromechanical boundary conditions, which significantly increase computational complexity [15-21].

Conventional finite element methods (FEM) have been extensively applied to FG piezoelectric and contact problems. However, FEM formulations require volumetric discretization of the entire domain, which can lead to large numbers of degrees of freedom, especially for multilayered or functionally graded configurations [20-24]. Moreover, mesh generation becomes increasingly demanding when dealing with thin layers, sharp material gradients, or evolving contact interfaces. These limitations motivate the development of alternative numerical approaches that can reduce modeling complexity while maintaining accuracy. Boundary-based methods, such as the boundary element method (BEM), offer attractive advantages by reducing the dimensionality of the problems [25-27]. Nevertheless, classical BEM formulations often face difficulties when applied to heterogeneous materials, multilayered structures, or problems involving domain integrals. To overcome these issues, the boundary-based finite element method (BFEM) has been proposed as a hybrid approach that combines the strengths of FEM and BEM [12, 14, 28]. In BFEM, each subdomain is modeled as a finite element constructed solely from boundary nodes, and the global system is assembled following standard finite element procedures. Previous studies have demonstrated the effectiveness of BFEM for anisotropic elastic plates, including problems with holes, cracks, and inclusions [29], as well as for stress analysis of functionally graded anisotropic plates with/without contact effects [12, 14, 28].

Despite these advances, the application of BFEM to piezoelectric plates, particularly those with multilayered or functionally graded configurations and contact interactions, has not yet been fully explored. The combined presence of electromechanical coupling, material heterogeneity, anisotropy, and contact constraints poses significant theoretical and numerical challenges that are not addressed by existing BFEM formulations. Motivated by this gap, the present study develops a boundary-based finite element method for analyzing stress and contact problems in multilayered and functionally graded piezoelectric plates. The plate is discretized into multiple material sublayers, each treated as an individual boundary-based finite element. The electromechanical coupling equations are formulated in terms of boundary tractions, electric displacements, and nodal forces, thereby avoiding volumetric discretization. Contact effects are incorporated through appropriate contact conditions, allowing the unknown contact regions and contact tractions to be determined as part of the solution. The accuracy and efficiency of the proposed approach are demonstrated through numerical examples and parametric studies examining the effects of material gradation, piezoelectric properties, and contact conditions.

The remainder of this paper is organized as follows. Section 2 presents multilayered and functionally graded anisotropic piezoelectric materials. Section 3 describes the BFEM formulation and its applications to the stress and contact analyses with multilayered/functionally graded piezoelectric materials. Numerical examples and parametric studies are provided in Section 4. Finally, conclusions are drawn in Section 5.

2. Multilayered and Functionally Graded Anisotropic Piezoelectric Materials

Multilayered and functionally graded (FG) piezoelectric plates are composed of multiple piezoelectric layers or continuously graded materials whose mechanical, electric, and piezoelectric properties vary through the thickness direction. Such configurations allow improved electromechanical performance, reduced interfacial stresses, and enhanced durability compared with homogeneous piezoelectric structures [1-5]. For multilayered piezoelectric plates (see Figure 1a), each layer is assumed to be homogeneous but may possess distinct anisotropic elastic, piezoelectric, and dielectric properties. Perfect bonding is assumed at the interfaces between adjacent layers, ensuring continuity of mechanical displacements and electric potential, as well as equilibrium of tractions and electric displacements. For functionally graded piezoelectric materials (see Figure 1b), the elastic, piezoelectric, and dielectric properties are assumed to vary continuously with position.

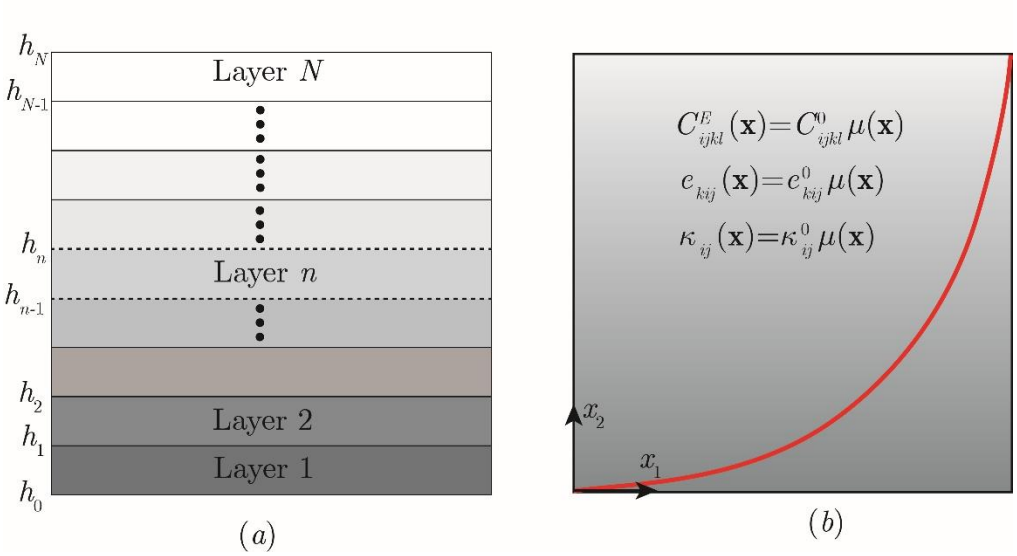

Figure 1. (*a*) Multilayered anisotropic piezoelectric plate (*b*) FG anisotropic piezoelectric plate.

The coupled electromechanical constitutive relations can be written as [1]

$$\sigma_{ij} = C^E_{ijkl}(\mathbf{x})\,\varepsilon_{kl} - e_{kij}(\mathbf{x})\,E_k, D_j = e_{jkl}(\mathbf{x})\,\varepsilon_{kl} + \kappa_{jk}(\mathbf{x})\,E_k, \quad (1)$$

where σ_{ij} and ε_{ij} denote the stresses and strains, respectively; D_j is the electric displacement, and E_k is the electric field. The strain and electric field are related to the mechanical displacement u_i, i=1,2,3, and the electric potential u_4 through $\varepsilon_{ij} = \frac{1}{2}\left(u_{i,j} + u_{j,i}\right)$ and $E_j = -u_{4,j}$. $\mathbf{x}$=(x_1, x_2) denotes the spatial coordinate. To describe the material gradation, the elastic stiffness, piezoelectric, and dielectric tensors are assumed to follow a grading function $\mu(\mathbf{x})$, such that

$$C^E_{ijkl}(\mathbf{x}) = C^0_{ijkl}\,\mu(\mathbf{x}), e_{kij}(\mathbf{x}) = e^0_{kij}\,\mu(\mathbf{x}), \kappa_{jk}(\mathbf{x}) = \kappa^0_{jk}\,\mu(\mathbf{x}), \quad (2)$$

where $\mu(\mathbf{x})$ may take piece-wise, linear, exponential, or polynomial forms, and C^0_{ijkl}, e^0_{kij}, and κ^0_{jk} are the corresponding material tensors at the reference position, e.g., the origin of the coordinate, as shown in Figure 1b.

Following the unified electromechanical formulation [18], the electric displacement and electric field are represented using extended stress and displacement variables by introducing $D_j = \sigma_{4j}$ and $-E_j = u_{4,j}$. With this definition, and by assuming vanishing body forces and free electric charges, the

coupled electromechanical behavior can be expressed in terms of an extended stress-strain relation. Under the assumptions of material symmetry, $\sigma_{ij} = \sigma_{ji}$, $\varepsilon_{ij} = \varepsilon_{ji}$, $u_{4,4} = 0$, and neglecting the higher-order coupling terms involving the fourth index, the basic equations can be rewritten in the compact form

$$\sigma_{ij} = C_{ijkl}(\mathbf{x})\,\varepsilon_{kl}, \varepsilon_{ij} = \frac{1}{2}\left(u_{i,j} + u_{j,i}\right), \sigma_{ij,j} = 0, i, j, k, l = 1,2,3,4. \tag{3}$$

This unified formulation allows the mechanical and electrical fields to be treated within a single theoretical framework and provides a convenient basis for applying BFEM, which is currently developed to solve problems with FG anisotropic elastic plates [12, 14, 28], to problems with multilayered/FG anisotropic piezoelectric plates.

3. Boundary-based Finite Element Method for Stress and Contact Analyses

3.1. Boundary-based finite element method

The boundary-based finite element method (BFEM) combines the advantages of the boundary element method and the finite element method by constructing finite elements using only boundary discretization [12, 14, 28]. In the BFEM, the computational domain is divided into several subregions (or layers), and each subregion is treated as an individual finite element, whose behavior is fully characterized by quantities defined on its boundary (see Figure 2). For each subregion, the governing equations of FG anisotropic piezoelectricity, expressed in the unified form introduced in Section 2, are solved using the BEM. This leads to explicit relations between the generalized boundary displacements and generalized boundary tractions without requiring volumetric discretization.

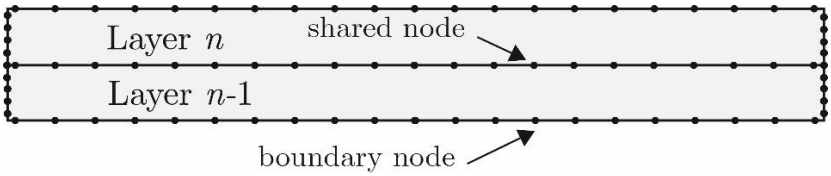

Figure 2. Discretization of sublayers in BFEM.

Let $\mathbf{u}_e^{(n)}$ and $\mathbf{t}_e^{(n)}$ denote the vectors of generalized nodal displacements, and generalized nodal tractions on the boundary of the n-th subregion, i.e.,

$$\mathbf{u}_e^{(n)} = (\mathbf{u}_1^{(n)}, \mathbf{u}_2^{(n)}, \ldots, \mathbf{u}_S^{(n)})^T, \mathbf{t}_e^{(n)} = (\mathbf{t}_1^{(n)}, \mathbf{t}_2^{(n)}, \ldots, \mathbf{t}_S^{(n)})^T \tag{4}$$

where S denotes the number of nodes on the n^{th} layer, which includes the shared nodes and boundary nodes; $\mathbf{u}^{(i)} = (u_1, u_2, u_3, u_4)^T$ and $\mathbf{t}^{(i)} = (t_1, t_2, t_3, t_4)^T$ and t_j is the traction component related to traction and the unit normal vector by $t_j = \sigma_{ij} n_i$, the BFEM formulation for each element can be expressed as

$$\mathbf{Y}_e^{(n)} \mathbf{u}_e^{(n)} = \mathbf{G}_e^{(n)} \mathbf{t}_e^{(n)}, \tag{5}$$

where $\mathbf{Y}_e^{(n)}$ and $\mathbf{G}_e^{(n)}$ are the boundary-based stiffness matrix of the element [12, 14, 28].

Knowing that the displacement field within each boundary-based element can be approximated using appropriate shape functions defined on the boundary, the generalized displacement inside the n-th element is interpolated as

$$\mathbf{u}^{(n)} = \mathbf{N}^{(n)}\mathbf{u}_e^{(n)}. \tag{6}$$

where $\mathbf{N}^{(n)}$ is the shape function matrix.

Applying the principle of minimum total potential energy with respect to the nodal displacements leads to the element equilibrium equation

$$\mathbf{K}_e^{(n)}\mathbf{u}_e^{(n)} = \mathbf{W}_e^{(n)}\,\mathbf{t}_e^{(n)} \tag{7}$$

where $\mathbf{W}_e^{(n)}$ is obtained by assembling the contributions of shape functions from all boundary elements [12, 14, 28] and $\mathbf{K}_e^{(n)}$ is the element stiffness matrix can be written explicitly as

$$\mathbf{K}_e^{(n)} = \mathbf{W}_e^{(n)}\left(\mathbf{G}_e^{(n)}\right)^{-1}\mathbf{Y}_e^{(n)}. \tag{8}$$

The stiffness matrices of all sublayers are then assembled following the standard finite element procedure to form the global system of equations. After solving for the generalized boundary displacements and tractions, the corresponding stress, strain, electric displacement, and displacement fields within each sublayer can be recovered using the associated boundary integral representations; further details can be found in Hwu [29].

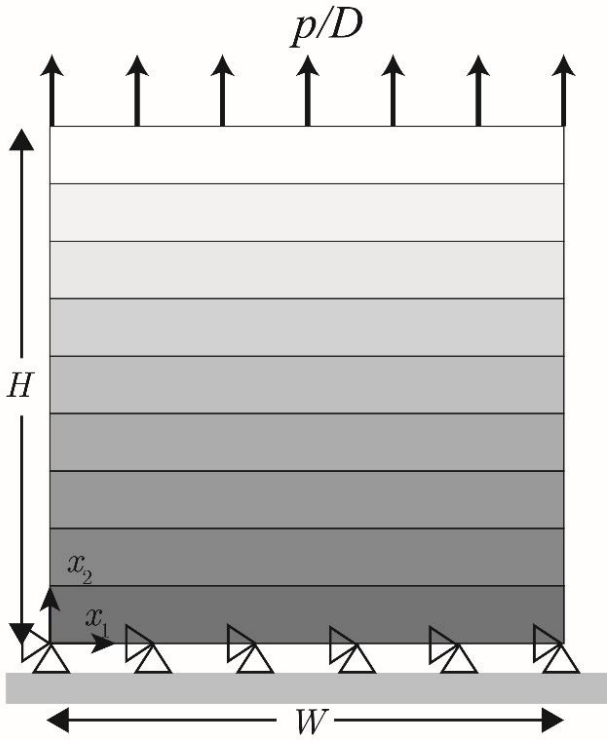

Figure 3. FG piezoelectric plate subjected to prescribed displacements/tractions/electric potentials and/or surface electric displacements. Here, *p/D* denotes uniform stress and/or electric displacement acting on the upper edge of the plate. The small triangles located at the bottom line denote the fixed displacements and the electric ground potential.

3.2. Application to Stress Analysis

For stress analysis, the BFEM formulation is applied under prescribed mechanical and electrical boundary conditions, such as prescribed displacements, tractions, electric potentials, or electric

displacements (see Figure 3). The global system of equations is assembled from (8) following the standard finite element assembly procedure by enforcing compatibility of generalized displacements and equilibrium of generalized tractions along the interfaces between adjacent subregions. This process leads to a global system of algebraic equations expressed entirely in terms of boundary nodal unknowns [28].

$$\mathbf{Kv}=\mathbf{p} \tag{9}$$

Once the global system of equations (9) is solved for the boundary nodal displacements and electric potentials, the corresponding boundary tractions and electric displacements can be recovered directly. The stress and electric displacement fields inside each subregion are then evaluated using the standard BEM [30].

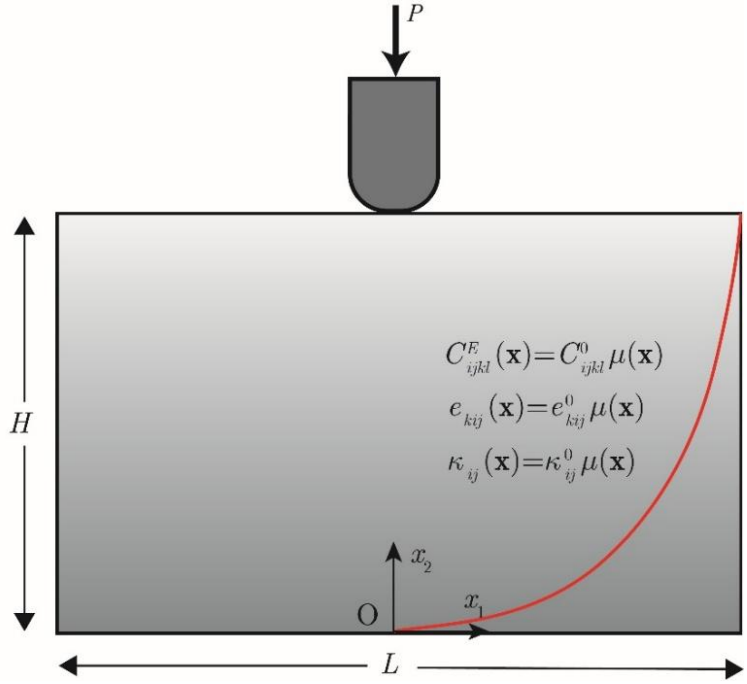

Figure 4. An FG anisotropic piezoelectric plate indented by a rigid parabolic punch. The punch is assumed to be an electrical insulator and is subjected to vertical load *P*. The lower boundary of the FGM plate is fixed.

3.3. Application for Contact Analysis

Unlike stress analysis, contact analysis focuses on determining the contact region as well as the associated contact tractions and surface deformations, which are generally unknown in advance. For simplicity, we consider the frictionless indentation of a rigid parabolic punch on an FG anisotropic piezoelectric plate, as shown in Figure 4. The punch is assumed to be an electrical insulator and is subjected to vertical load *P*. To apply the BFEM to the contact problem, equation (8) is applied to each layer and then assembled according to the standard rule of FEM. By dividing the boundary nodes into contact nodes and non-contact nodes, we obtain the following systems of linear equations from BFEM

$$\mathbf{K}^{(c)}\mathbf{u}^{(c)}+\mathbf{K}^{(nc)}\mathbf{u}^{(nc)}=\mathbf{W}^{(c)}\mathbf{t}^{(c)}+\mathbf{W}^{(nc)}\mathbf{t}^{(nc)}, \tag{10}$$

where (*c*) and (*nc*) denote the values and coefficients related to the contact and non-contact regions. Like the problems with anisotropic FG plates [14], the contact nodes are designated as the nodes along the region under the punch, and the non-contact nodes, including all the remaining nodes. If we further

divide the non-contact nodes into those with displacement prescribed ($\mathbf{u}_p^{(nc)}, \mathbf{t}_u^{(nc)}$) and those with traction prescribed ($\mathbf{u}_u^{(nc)}, \mathbf{t}_p^{(nc)}$), where the subscripts u and p denote the unknown and prescribed values, equation (10) can be rewritten as

$$\mathbf{H}^{(nc)}\mathbf{x}^{(nc)} + \mathbf{K}^{(c)}\mathbf{u}^{(c)} - \mathbf{W}^{(c)}\mathbf{t}^{(c)} = \mathbf{f}, \tag{11a}$$

where

$$\mathbf{H}^{(nc)} = \left[\mathbf{K}_u^{(nc)} - \mathbf{W}_u^{(nc)}\right], \quad \mathbf{x}^{(nc)} = \begin{Bmatrix} \mathbf{u}_u^{(nc)} \\ \mathbf{t}_u^{(nc)} \end{Bmatrix}, \quad \mathbf{f} = -\mathbf{K}_p^{(nc)}\mathbf{u}_p^{(nc)} + \mathbf{W}_p^{(nc)}\mathbf{t}_p^{(nc)}. \tag{11b}$$

Equation (11a) contains $4n_c$+$4n_{nc}$ equations with $4n_c$+$8n_{nc}$ unknowns. To have a complete system of equations, we need additional equations that come from contact constraint relations and equilibrium conditions of the punch.

For the insulating punch considered in this paper, the contact constraint relations can be written as follows for two different modes of each contact node [14, 18]

Separation:

$$t_1 = t_2 = t_3 = t_4 = 0. \tag{12}$$

Contact:

$$t_1 = 0,\ u_2 = \delta_p,\ t_3 = 0,\ t_4 = 0, \tag{13}$$

where δ_p is the rigid body motion of the flat-ended punch. Since the contact modes of the contact nodes are usually unknown, we first assume all the contact nodes are either in contact or in separation. Applying equations (12) or (13) to these nodes and assembling them, we have

$$\mathbf{R}_u\mathbf{u}^{(c)} + \mathbf{R}_t\mathbf{t}^{(c)} + \mathbf{R}_p\delta_p = \mathbf{f}_c, \tag{14}$$

Equation (14) relates the unknown boundary displacements and tractions under the prescribed contact constraints. To complete the formulation, the global equilibrium condition of the punch must be satisfied. This requirement leads to

$$\mathbf{D}_q\mathbf{t}_2^c = P. \tag{15}$$

By combining Eqs. (11a), (14) and (15), a solvable system of linear equations is established, i.e.,

$$\begin{bmatrix} \mathbf{H}^{(nc)} & \mathbf{K}^{(c)} & -\mathbf{W}^{(c)} & \mathbf{0} \\ \mathbf{0} & \mathbf{R}_u & \mathbf{R}_t & \mathbf{R}_p \\ \mathbf{0} & \mathbf{0} & \mathbf{D}_q & \mathbf{0} \end{bmatrix} \begin{Bmatrix} \mathbf{x}^{(nc)} \\ \mathbf{u}^{(c)} \\ \mathbf{t}^{(c)} \\ \delta_p \end{Bmatrix} = \begin{Bmatrix} \mathbf{f} \\ \mathbf{f}_c \\ P \end{Bmatrix}. \tag{16}$$

Solving (16), the contact solution can be uniquely determined. It should be emphasized that equation (14) is derived based on the initially assumed contact modes of all nodes within the potential contact region. Consequently, an iterative procedure is required to verify and update the contact conditions. During the iterative process, both the contact region and the corresponding contact tractions are successively updated until convergence is achieved [12, 14, 28]. Once convergence is reached, the BFEM solution provides the contact pressure distribution, the associated contact tractions, and the coupled electromechanical response of the piezoelectric plate. Owing to its boundary-only discretization and its capability to consistently account for anisotropy, material gradation, and electromechanical

coupling, the proposed contact-BFEM formulation is particularly well suited for the analysis of contact problems in multilayered and functionally graded piezoelectric plates.

4. Results and Discussion

4.1. Stress Analysis with an FG Piezoelectric Plate

To validate the proposed BFEM formulation, we first consider an FG anisotropic piezoelectric plate subjected to a tension load p as illustrated in Figure 3. The load p is specified as p= 10 (kN/m^2). The plate has width W=10 (cm) and height H=10 (cm), and is composed of an anisotropic functionally graded piezoelectric (FGP) plate as defined in equation (2). The reference material properties are selected to be PZT-7A as shown in equation (17) and vary according to an exponential rule, i.e, $\mu(\mathbf{x}) = \mu(x_2) = e^{\beta x_2}$.

$$\begin{aligned} &C_{11}^0 = C_{33}^0 = 148, C_{12}^0 = C_{23}^0 = 74.2, C_{13}^0 = 76.2, C_{22}^0 = 131, \\ &C_{44}^0 = C_{66}^0 = 25.4, C_{55}^0 = 55.9 \text{ (unit: GPa), others } C_{ij}^0 = 0, \\ &i, j = 1,2,3,4,5,6, \end{aligned} \tag{17a}$$

and

$$\begin{aligned} &e_{21}^0 = e_{23}^0 = -2.1, e_{22}^0 = 9.5,\ e_{16}^0 = e_{24}^0 = 9.7 \text{ (unit: C/m}^2), \\ &\text{others } e_{ij}^0 = 0,\ i = 1,2,3,\ j = 1,2,3,4,5,6, \end{aligned} \tag{17b}$$

and

$$\kappa_{11}^0 = \kappa_{33}^0 = 8.11, \kappa_{22}^0 = 7.35, \text{ (unit: } 10^{-9}\text{ C/Vm), others } \kappa_{ij}^0 = 0,\ i, j = 1,2,3. \tag{17c}$$

In the above, C_{ij}^0, e_{ij}^0 and κ_{ij}^0 are the contract notation of the elastic stiffness, piezoelectric, and dielectric tensors shown in equations (1) and (2) [30]. To simulate the FGM material by BFEM, we divide the plate into N layers (see Figure 3). Each layer has a homogeneous material whose material are $\bar{C}_{ijkl}^{(n)}$, $\bar{e}_{kij}^{(n)}$ and $\bar{\kappa}_{ij}^{\varepsilon(n)}$ and are evaluated by the following rule

$$\begin{aligned} &\bar{C}_{ijkl}^{(n)} = \frac{1}{\Delta h_n}\int_{h_{n-1}}^{h_n} C_{ijkl}^0 \mu(x_2) dx_2,\ \bar{e}_{ij}^{(n)} = \frac{1}{\Delta h_n}\int_{h_{n-1}}^{h_n} e_{ij}^0 \mu(x_2) dx_2, \\ &\bar{\kappa}_{ij}^{\varepsilon(n)} = \frac{1}{\Delta h_n}\int_{h_{n-1}}^{h_n} \kappa_{ij}^0 \mu(x_2) dx_2,\ n = 1,2,...,N, \end{aligned} \tag{18}$$

where n denotes the n^{th} layer and Δh_n denotes the n^{th} layer thickness.

Figures 5, 6, 7, and 8 present the variation of the displacement and electric potential along the left edge of the plate with different layer numbers N for the different gradation ratios β, i.e., β=0 and 1. For the case β=0, the FG piezoelectric plate is homogeneous. As expected, the number of layers does not affect the results. However, for β=1, the numerical results indicate that as the number of layers increases, the solution converges. This behavior is consistent with the expected response of functionally graded materials, in which a finer layer discretization yields a more accurate approximation of the continuous material variation.

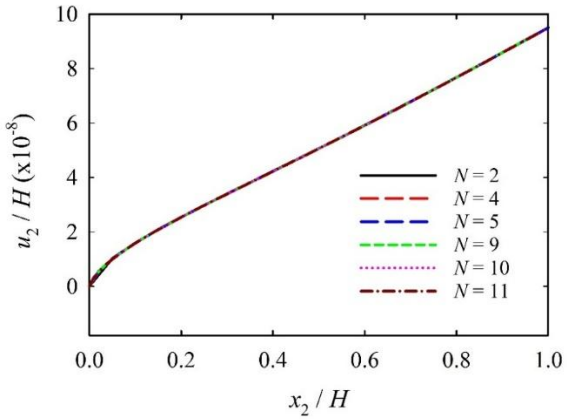

Figure 5. Displacement in the x_2 direction on the left edge of the FG plate for β=0.

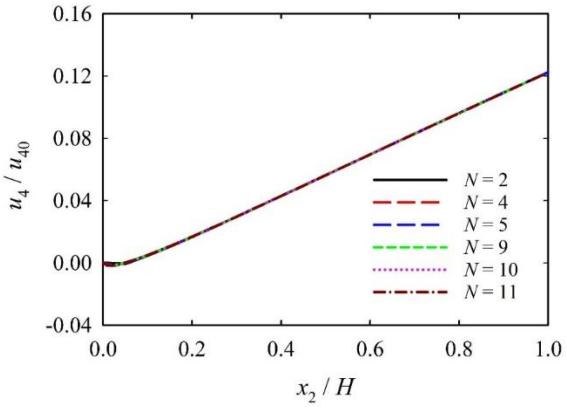

Figure 6. Electric potential on the left edge of the FG plate for β=0. Here u_{40}=1 (kV).

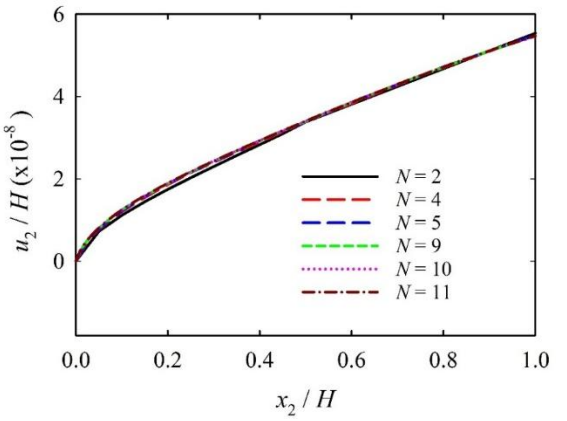

Figure 7. Displacement in the x_2 direction on the left edge of the FG plate for β=1.

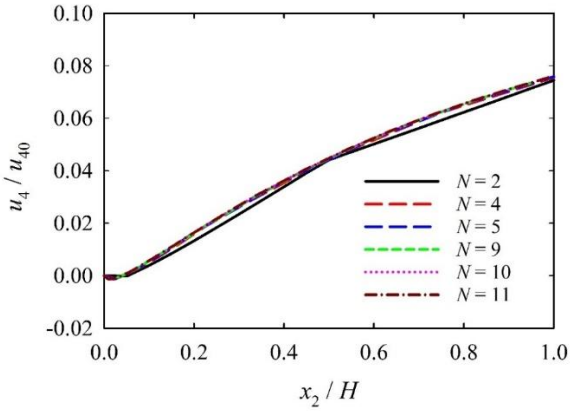

Figure 8. Electric potential on the left edge of the FG plate for β=1. Here u_{40}=1 (kV).

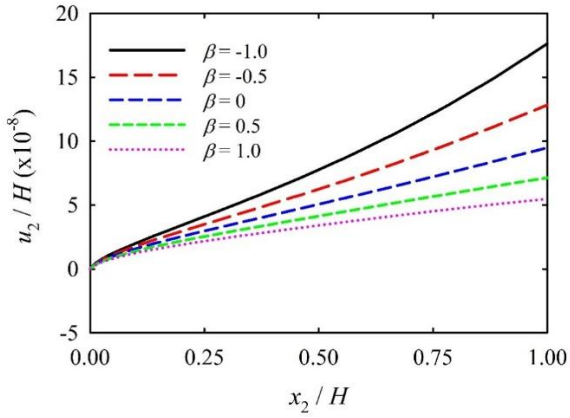

Figure 9. Displacement in the x_2 direction on the left edge of the FG plate for different values of β.

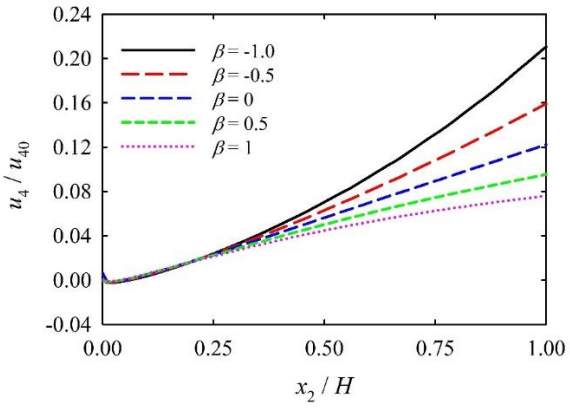

Figure 10. Electric potential on the left edge of the FG plate for different values of β. Here, u_{40}=1 (kV).

To study the influence of the gradation β, we vary its value as β=-1, -0.5, 0, 0.5, 1, and plot Figures 9 and 10, which show the variation of the displacement and electric displacement on the left boundary. From the figure, we see that as the graded constant β increases, the displacement u_2 and the electric potential u_4 both decrease. The graded property significantly affects the plate's mechanical and electrical responses.

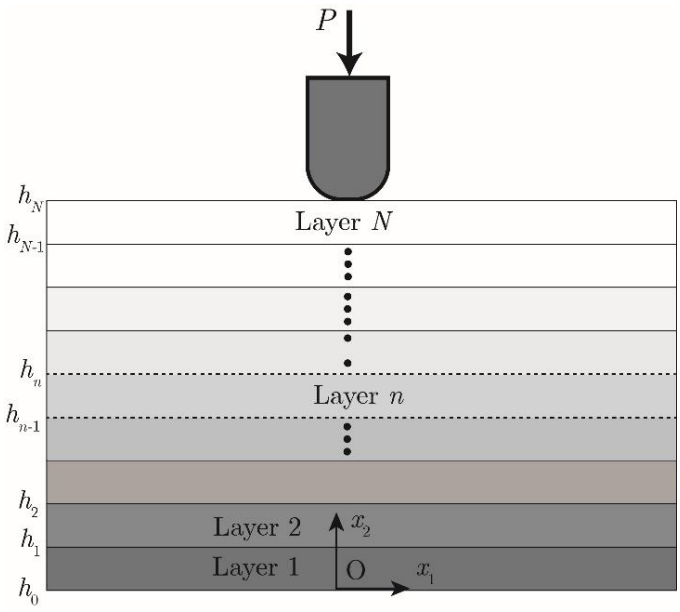

Figure 11. Simulate the indentation of the FGM plate in BFEM.

4.2. Contact Analysis with FG Piezoelectric Plates

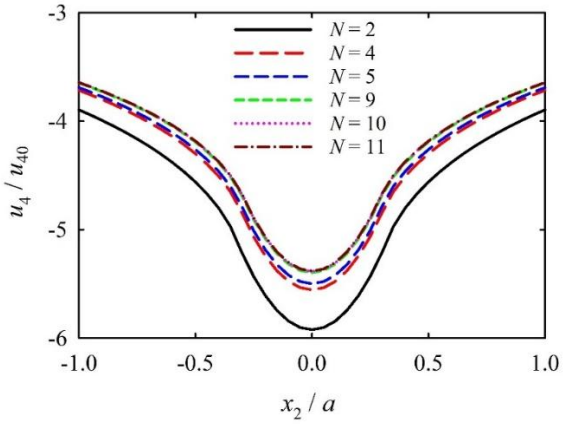

Figure 12. Electric potential along the top surface of the FG piezoelectric plate. Here u_{40}=10 (kV).

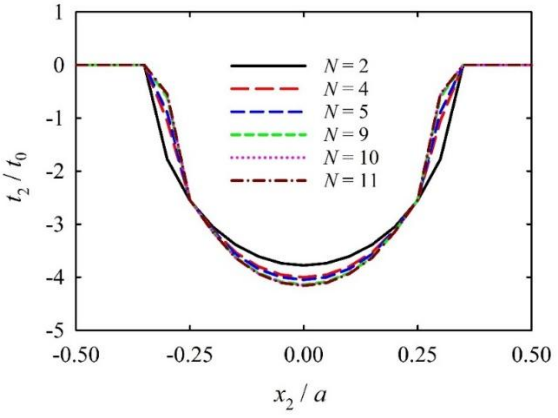

Figure 13. Stress distributions beneath the punch. Here, $t_0 = 100$ (MPa).

To investigate the performance of the proposed BFEM formulation in contact problems, we consider an FG anisotropic piezoelectric plate subjected to frictionless contact with a parabolic rigid indenter, as shown in Figure 4. The punch has a width of 0.04 (cm), and its head is described as $f(x_1)=x_1^2/2R$, where

R=20 (cm). The load applied on the punch is assumed to be P= 4 (kN/m). The plate geometry and the FG piezoelectric material are identical to those used in the previous section. To simulate the FGM plate, we divide it into N sublayers as shown in Figure 11. Each layer except the top one was discretized using 224 nodes. For the top layer, 300 nodes were adopted to obtain acceptable results in the contact analysis.

Figures 12 and 13 present the electric potential and stress distributions beneath the punch for different numbers of sublayers. To obtain the results in these figures, the gradation ratio β is set to be 1. Similar to the observations in Section 4.1, the results demonstrate convergence as the number of layers increases. When only a small number of sublayers is used, slight discrepancies can be observed. As the discretization is refined, these differences gradually diminish, and the solutions become nearly indistinguishable. This behavior confirms that the layered approximation provides a stable and reliable representation of the continuously graded material. Based on the observations, a layer count of N=9 is used to obtain the contact results in the following sections.

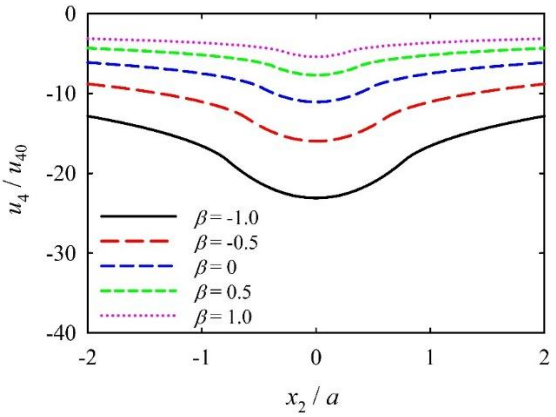

Figure 14. Electric potential along the top surface of the FG piezoelectric plate for different values of gradation ratio β. Here u_{40}=10 (kV).

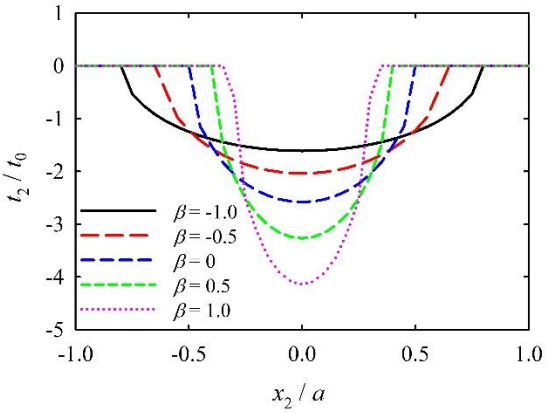

Figure 15. Stress distributions beneath the punch for different values of the gradation ratio β. Here $t_0 = 100$ (MPa).

Influence of the material gradation

To study the influence of material gradation on the contact responses, we vary the gradation ratio β as in Section 4.1 and plot Figures 14 and 15, which show the variation of the electric potential and contact stress accordingly. From these figures, we see that material gradation has a pronounced influence on the electrical and mechanical contact responses. Plates with increasing stiffness toward the contact surface exhibit higher peak contact pressures and smaller contact regions. Conversely, softer gradation leads to reduced pressure concentrations and enlarged contact zones. These trends are physically consistent with the stiffness variation induced by the functional grading. As to the electric potential, the magnitude of the electric potential reduces when the gradation ratio β increases. In conclusion, the functional grading modifies both the mechanical field and the coupled electrical field, which therefore should be carefully considered in designing FGM structures with electromechanical coupling effects.

Influence of the material anisotropy

To study the influence of material anisotropy on the contact responses, the material coordinate system is rotated according to equation (17) by an angle γ about the x_3-axis. Figures 16 and 17 present the variations of the electric potential and contact traction for different values of γ, respectively. To obtain the results in these figures, we also set the gradation ratio β to be 1. From Figure 16, it can be observed that the electric potential is highly sensitive to the material orientation. As the rotation angle

γ increases, both the magnitude and the distribution pattern of the electric potential change significantly. For $\gamma = 0°$ and $30°$, the electric potential remains negative over the entire contact region and reaches its minimum value near the center beneath the punch. When $\gamma = 60°$, the negative magnitude is noticeably reduced. For $\gamma = 90°$, the electric potential becomes positive over a large portion of the domain and exhibits a completely different distribution trend. This clearly demonstrates that the electromechanical coupling response is strongly dependent on the anisotropic orientation of the material. In contrast, Figure 17 shows that the contact traction distribution is only moderately affected by the rotation angle. As γ increases, the peak compressive traction slightly decreases, while the overall symmetric shape of the contact pressure profile remains nearly unchanged. The size of the contact region is almost unaffected by the rotation. This indicates that the mechanical stiffness variation induced by material rotation modifies the magnitude of the contact stress but does not significantly alter the overall pressure pattern. These results suggest that for the present FG piezoelectric materials, the material anisotropy has a more pronounced influence on the electrical response than on the mechanical contact response. The strong sensitivity of the electric potential arises from the rotation-induced transformation of the piezoelectric coefficients and dielectric constants, which directly affects the coupled electromechanical fields under contact loading.

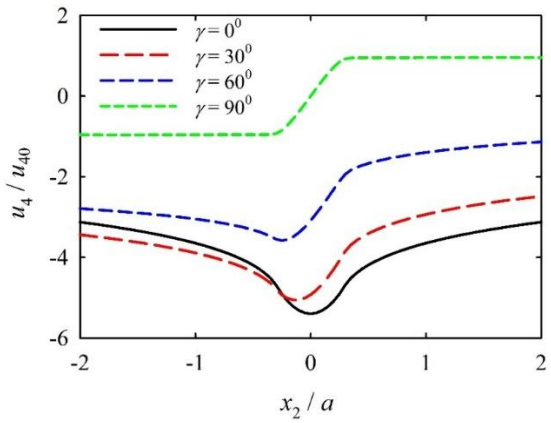

Figure 16. Electric potential along the top surface of the FG piezoelectric plate for different rotation angles γ. Here u_{40}=10 (kV).

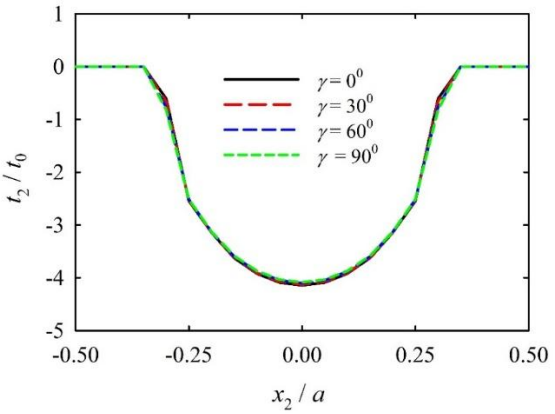

Figure 17. Stress distributions beneath the punch for different values of rotation angle γ. Here $t_0 = 100$ (MPa).

5. Conclusions

A boundary-based finite element method (BFEM) has been developed for the analysis of stress and contact problems in multilayered and functionally graded piezoelectric plates. In the proposed formulation, the plate domain is discretized into material sublayers, each represented by a boundary-based finite element. By establishing direct relationships between boundary tractions, electric displacements, and nodal forces, the coupled electromechanical governing equations are transformed into a boundary-based framework, eliminating the need for volumetric discretization. The formulation has been extended to contact problems by incorporating the contact constraints directly into the BFEM system equations. This treatment enables the unknown contact regions and contact tractions to be determined as part of the solution without introducing additional domain variables. The method

naturally accommodates multilayered configurations, continuous material gradation, anisotropy, and electromechanical coupling effects. Numerical examples demonstrate that the proposed approach provides accurate and stable solutions. Convergence studies show that the layered approximation effectively captures the behavior of functionally graded materials, with the solutions becoming insensitive to further refinement beyond a sufficient number of sublayers. Parametric investigations further illustrate the significant roles of material gradation and anisotropic properties in governing the electromechanical responses of the plates. Overall, the BFEM formulation offers an efficient and reliable alternative for the analysis of coupled electromechanical problems, particularly for functionally graded and layered piezoelectric structures. Although the method has the mentioned advantages, the present study is limited to two-dimensional problems and assumes a frictionless, electrically insulating punch in the contact analysis. These aspects will be considered in future work.

Acknowledgments

This study would like to acknowledge the funding by the Project code QG.24.119 of the Science and Technology Development Fund of Vietnam National University Hanoi.

References

[1] Z. Yin, J. Zhang, F. Yang, W. Ye, J. Liu, G. Lin**,** An Efficient Scaled Boundary Finite Element Approach in Bending and Buckling Analysis of Functionally Graded Piezoelectric Plates, Engineering Analysis with Boundary Elements, Vol. 132, 2021, pp. 168-181, https://doi.org/10.1016/j.enganabound.2021.07.015.

[2] X.B. Yan, S.M. Liu, P.H. Wen, J. Sladek, V. Sladek, Homogeneous and Functionally Graded Piezoelectric Structure Analysis with Finite Block Method, Composite Structures, Vol. 365, 2025, pp. 119188, https://doi.org/10.1016/j.compstruct.2025.119188.

[3] Z. Su, G. Jin, T. Ye, Electro-mechanical Vibration Characteristics of Functionally Graded Piezoelectric Plates with General Boundary Conditions, International Journal of Mechanical Sciences, Vol. 138-139, 2018, pp. 42-53, https://doi.org/10.1016/j.ijmecsci.2018.01.040.

[4] J. Yang, H. J. Xiang, Thermo-electro-mechanical Characteristics of Functionally Graded Piezoelectric Actuators, Smart Materials and Structures, Vol. 16, 2007, pp. 784, https://doi.org/10.1088/0964-1726/16/3/028.

[5] C. C. M. Wu, M. Kahn, W. Moy, Piezoelectric Ceramics with Functional Gradients: a New Application in Material Design, Journal of the American Ceramic Society, Vol. 79, 1996, pp. 809-812, https://doi.org/10.1111/j.1151-2916.1996.tb07951.x.

[6] X. F. Li, X. L. Peng, K. Y. Lee, Radially Polarized Functionally Graded Piezoelectric Hollow Cylinders as Sensors and Actuators, European Journal of Mechanics - A/Solids, Vol. 29, No. 4, 2010, pp. 704-713, https://doi.org/10.1016/j.euromechsol.2010.02.003.

[7] H. L. Dai, L. Hong, Y. M. Fu, X. Xiao, Analytical Solution for Electromagnetothermoelastic Behaviors of a Functionally Graded Piezoelectric Hollow Cylinder, Applied Mathematical Modelling, Vol. 34, No. 2, 2010, pp. 343-357, https://doi.org/10.1016/j.apm.2009.04.008.

[8] A. L. Shuvalov, E. L. Clezio, G. Feuillard, The State-vector Formalism and the Peano-series Solution for Modelling Guided Waves in Functionally Graded Anisotropic Piezoelectric Plates, International Journal of Engineering Science, Vol. 46, No. 9, 2008, pp. 929-947, https://doi.org/10.1016/j.ijengsci.2008.03.007.

[9] M. K. Pal, A. K. Singh, Analysis of Reflection and Transmission Phenomenon at Distinct Bonding Interfaces in a Rotating Pre-stressed Functionally Graded Piezoelectric-Orthotropic Structure, Analysis of Reflection and Transmission Phenomenon at Distinct Bonding Interfaces in a Rotating Pre-stressed Functionally Graded Piezoelectric-Orthotropic Structure, Vol. 409, 2021, pp. 126398, https://doi.org/10.1016/j.amc.2021.126398.

[10] F. Li, J. Xie, O. Shi, Multilayer Homogeneous Model for Functionally Graded Piezoelectric Structure with Arbitrary Property: From Mechanical Analysis to Optimization, Composite Structures, Vol. 384, 2026, pp. 120173, https://doi.org/10.1016/j.compstruct.2026.120173.

[11] W. K. Zhang, C. Lu. C. Y. Fan, M. H. Zhao, H. Y. Dang, Axisymmetric Interfacial Analysis of Functionally Graded Piezoelectric Semiconductor Films Incorporating Surface Effects, Thin-Walled Structures, Vol. 218, 2026, pp. 114130, https://doi.org/10.1016/j.tws.2025.114130.
[12] T. K. H. Nguyen, V. T. Nguyen, V. L. Nguyen, X. T. Nguyen, Pin-Loaded Hole Contact in Anisotropic Multi-Layered/Functionally Graded Composite Plate, Composite Structures, Vol. 382, 2026, pp. 120103, https://doi.org/10.1016/j.compstruct.2026.120103.
[13] S. Jie, L. L. Ke, Y. S. Wang, Axisymmetric Frictionless Contact of a Functionally Graded Piezoelectric Layered Half-Space Under a Conducting Punch, International Journal of Solids and Structures, Vol. 90, 2016, pp. 45-59, https://doi.org/10.1016/j.ijsolstr.2016.04.011.
[14] X. T. Nguyen, V. T. Nguyen, N. D. Duc. Indentation on Multilayered and Functionally Graded Anisotropic Elastic Plates, Acta Mechanica, 2026, https://doi.org/10.1007/s00707-026-04658-w.
[15] B. Yang, E. Pan, V. K. Tewary, Static Responses Of A Multilayered Anisotropic Piezoelectric Structure To Point Force And Point Charge, Smart Materials and Structures, Vol. 13, 2003, pp. 175, https://doi.org/10.1088/0964-1726/13/1/020.
[16] Y. T. Zhou, K. Y. Lee, Frictional Contact of Anisotropic Piezoelectric Materials Indented by Flat and Semi-Parabolic Stamps, Archive of Applied Mechanics, Vol. 83, 2013, pp. 73-95, https://doi.org/10.1007/s00419-012-0633-5.
[17] Y. T. Zhou, K. Y. Lee, Theory of Moving Contact of Anisotropic Piezoelectric Materials via Real Fundamental Solutions Approach, European Journal of Mechanics - A/Solids, Vol. 35, 2012, pp. 22-36, https://doi.org/10.1016/j.euromechsol.2012.01.001.
[18] V. T. Nguyen, V. S. Pham, N. D. Duc, T. Q. Bui, Semi-analytical Method for Frictional Sliding Contact of a Piezoelectric Layer-Substrate, Mechanics of Materials, Vol. 213, 2026, pp. 105572, https://doi.org/10.1016/j.mechmat.2025.105572.
[19] V. T. Nguyen, T. K. H. Nguyen, C. M. Nguyen, Semi-Analytical Method for Pin-Loaded Joint Contact in Anisotropic Piezoelectric Plates, International Journal of Mechanical Sciences, Vol. 288, 2025, pp. 110001, https://doi.org/10.1016/j.ijmecsci.2025.110001.
[20] J. Sladek, V. Sladek, H. H. -H. Lu, D. L. Young, The FEM Analysis of FGM Piezoelectric Semiconductor Problems, Composite Structures, Vol. 163, 2017, pp. 13-20, https://doi.org/10.1016/j.compstruct.2016.12.019.
[21] X. Q. He, K. M. Liew, T. Y. Ng, S. Sivashanker, A FEM Model for the Active Control of Curved FGM Shells Using Piezoelectric Sensor/Actuator Layers, International Journal for Numerical Methods in Engineering, Vol. 54, 2002, pp. 853-870, https://doi.org/10.1002/nme.451.
[22] M. N. Balci, S. Dag, B. Yildirim, Subsurface Stresses in Graded Coatings Subjected to Frictional Contact with Heat Generation, Journal of Thermal Stresses, Vol. 40, 2016, pp. 517-534, https://doi.org/10.1080/01495739.2016.1261261.
[23] M. A. Güler, A. Kucuksucu, K. B. Yilmaz, B. Yildirim, On the Analytical and Finite Element Solution of Plane Contact Problem of a Rigid Cylindrical Punch Sliding Over a Functionally Graded Orthotropic Medium, International Journal of Mechanical Sciences, Vol. 120, pp. 2017, pp. 12-29, https://doi.org/10.1016/j.ijmecsci.2016.11.004.
[24] X. Tang, W. Yang, J. Liu, K. Qi. A High-Efficiency Versatile Adhesive Contact Model for Layered Media. Tribology International, Vol. 212, 2025, pp. 110926, https://doi.org/10.1016/j.triboint.2025.110926.
[25] Y. Liu, H. Fan, Analysis of Thin Piezoelectric Solids by the Boundary Element Method, Computer Methods in Applied Mechanics and Engineering, Vol. 191, No. 21-22, 2002, pp. 2297-2315, https://doi.org/10.1016/S0045-7825(01)00410-8.
[26] V. L. Nguyen, V. T. Nguyen, N. D. Duc, Pin-loaded Hole Contact in an Anisotropic Magnetoelectroelastic Plate, International Journal of Mechanical Sciences, Vol. 302, 2025, pp. 110551, https://doi.org/10.1016/j.ijmecsci.2025.110551.
[27] V. T. Nguyen, C. Hwu, Boundary Element Method for Two-Dimensional Frictional Contact Problems of Anisotropic Elastic Solids, Engineering Analysis with Boundary Elements, Vol. 108, 2019, pp. 49-59, https://doi.org/10.1016/j.enganabound.2019.08.010.
[28] X. T. Nguyen, V. T. Nguyen, N. D. Duc, Boundary-Based Finite Element Method for Anisotropic Functionally Graded Materials, Engineering Analysis with Boundary Elements, Vol. 181, 2025, pp. 106526, https://doi.org/10.1016/j.enganabound.2025.106526.
[29] C. Hwu, S. T. Huang, C. C. Li, Boundary-Based Finite Element Method for Two-Dimensional Anisotropic Elastic Solids with Multiple Holes and Cracks, Engineering Analysis with Boundary Elements, Vol. 79, 2017, pp. 13-22, https://doi.org/10.1016/j.enganabound.2017.03.003.
[30] C. Hwu, Anisotropic Elasticity with Matlab, Springer Cham, 2021.